

# *Research on layout optimization of heliostat based on the Fresnel equation*

Zhenxiang Zhao\*, Jiayi Li, Xinyue Xu

Shenzhen MSU-BIT University, Shenzhen, 518172, China

\*Corresponding author: zzx15228749650@outlook.com

**Keywords:** Optical model; Fresnel equation; Multi-target genetic algorithm; Heliostat field

**Abstract:** This study focuses on optimizing the layout of a tower heliostat field for solar thermal power generation. It explores key parameters related to heliostat positioning, installation height, size, and absorption tower positioning. Through comprehensive modeling and analysis, the optimal layout parameters are determined under various conditions. The study developed separate optical models for shadow occlusion efficiency, cosine efficiency, and collector stage efficiency, based on the Fresnel equation and relevant functions, using MATLAB. The findings reveal that the optimal absorption tower position is (0, 0) with a size of 6m \* 6m, resulting in an annual average thermal power output of 77.0717 MW and an annual average thermal power output per unit mirror area of 1.2269 kW/m<sup>2</sup>. Further optimization using a genetic algorithm with 500 iterations led to an absorber position of (0, 0), with a size of 7m \* 7m and 1,052 facets, resulting in an annual thermal power output of 61.1795 MW and an annual thermal power per unit mirror area of 1.0722 kW/m<sup>2</sup>. The study also assessed the model's robustness and sensitivity, demonstrating its reliability in complex real-world scenarios.

## 1. Introduction

In the context of the global push for clean and low-carbon energy solutions, solar thermal power generation has witnessed significant advancements in recent years due to its characteristics of environmental protection, stability, adjustability and easy grid connection<sup>[1][2]</sup>. Among the various solar thermal power generation systems, the tower solar thermal power station has the characteristics of substantial light concentration, minimal heat loss, large system capacity, and high power generation efficiency<sup>[3]</sup>. However, it's important to note that the construction cost of the heliostat field in a tower solar thermal power station typically constitutes a substantial portion, ranging from 30% to 50% of the overall investment in the power station<sup>[4]</sup>. Furthermore, the associated efficiency losses can be as high as 30% to 40%. Consequently, optimizing the layout of a high-efficiency, cost-effective heliostat field has emerged as a significant and active research area. Building on this premise, this paper studies the annual average optical efficiency, annual average cosine efficiency, annual average shadow occlusion efficiency, annual average cut efficiency and annual average output thermal power per unit mirror area, further studies how to lay the heliostat field to the unit mirror area annual average output thermal power and the installation height of the same, solve the optimal parameters: absorption tower position coordinates, heliostat position, size, quantity and installation

height, to maximize the average annual output thermal power of the unit mirror area [5].

## 2. Study of the optical efficiency of the heliostatic field

If the height of the planned absorber is 80 m, and the collector adopts a cylindrical outer light collector with a height of 8 m and a diameter of 7 m. No heliostat is installed within 100 m around the absorption tower, and open space is set aside to build a workshop for installing power generation, energy storage, control and other equipment. The shape of the heliostat is a flat rectangle, and its upper and lower sides are always parallel to the ground. The distance between the two sides is called the mirror height, and the distance between the left and right sides of the mirror is called the mirror width. Usually, the mirror width is not less than the mirror height. The side length of the mirror is between 2 m and 8 m, and the mounting height is between 2 m and 6 m. The mounting height must ensure that the mirror does not touch the ground when rotating around the horizontal axis. Due to the need for maintenance and cleaning of the vehicle, the distance between the center of the adjacent heliostat base is more than 5 m than the width of the mirror.

It is planned to build a circular heliostat field in the circular area of east longitude 98.5,39.4 N 3,3000 m and a radius of 350 m (Fig 2). The coordinate system is established with the center of the circular area as the origin, the east direction as the x-axis, the north direction as the y-axis, and the vertical direction of the ground as the z-axis. Using Python visualization to obtain the following heliograph layout (left, top), as shown in Fig 1, 2.

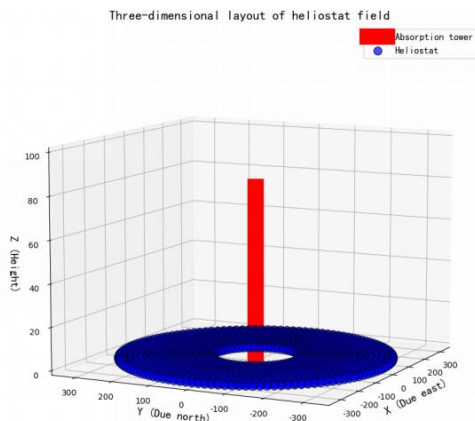


Figure 1: Heliostat field layout left (overall)

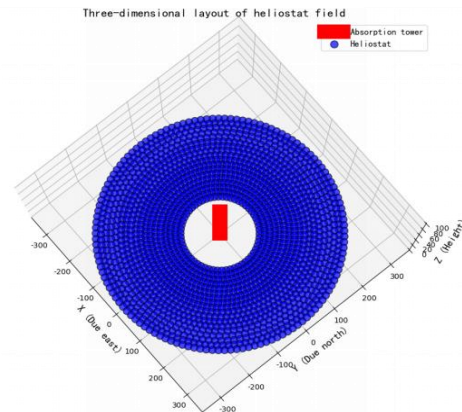


Figure 2: Heliostat field layout right (top)

### 2.1 Model building

In the first case of shadow occlusion loss, the occlusion of the incoming rays between adjacent heliostats is shown in Fig 3.

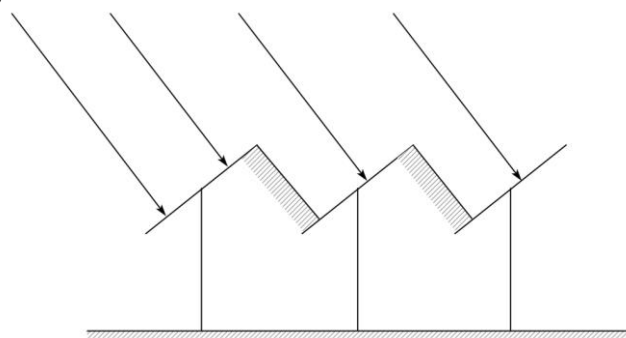


Figure 3: Occlusion of the sun's light between the heliostat

According to the light projection law, the occlusion efficiency of the incident light line  $\eta_{sb}$  is obtained [6].

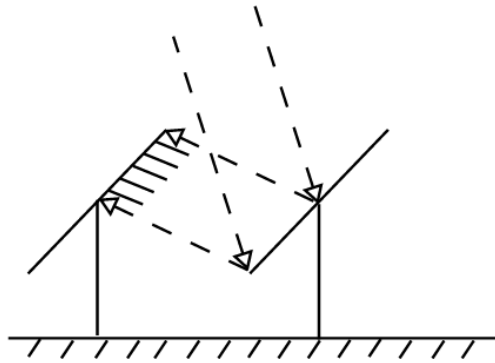
$$\eta_{sb} = \frac{d \tan \alpha}{n \cos \alpha_h (\tan \alpha_s + \tan \alpha_h)} \quad (1)$$

$d$  is the center spacing between two heliographs,  $\alpha_s$  is the height Angle of the sun,  $\alpha_h$  is the elevation Angle of the heliostat, and  $n$  is the width of the heliostat [7].

From the mathematical knowledge, it is concluded that.

$$\alpha_h = \frac{\pi}{2} - \alpha_s \quad (2)$$

In the second case of shadow occlusion loss, the occlusion of adjacent heliostats against each other is shown in Fig 4.



2Figure 4: Occlusion of the reflected light

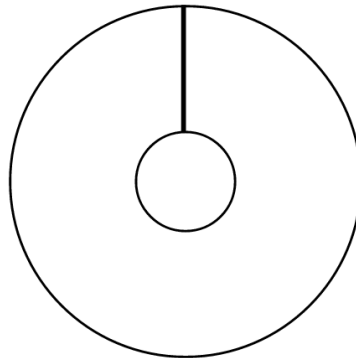
The plane equation of the adjacent mirror element is.

$$Z = k_{j+1}X - k_{j+1}X_{aj+1} \quad (3)$$

$k_{j+1} = \tan \beta_{j+1}$  is the slope of the adjacent mirror element  $\beta_{j+1}$  is the inclination angle of the  $j$ th+1st mirror element.

If the reflected light is within the aperture of the mirror element, the light cannot reach the receiver due to occlusion.

In the third case of shadow occlusion loss, the tower shadow shields the heliostat field. Since the diameter of the tower is not indicated in this paper, the diameter of the tower  $d = 2\text{m}$  is shown in Fig 5.



3Figure 5: Schematic diagram of the maximum tower column shadow

$$\text{Maximum shadow occlusion rate of tower columns} = \frac{4(R-r)}{\pi R^2 - \pi r^2} \quad (4)$$

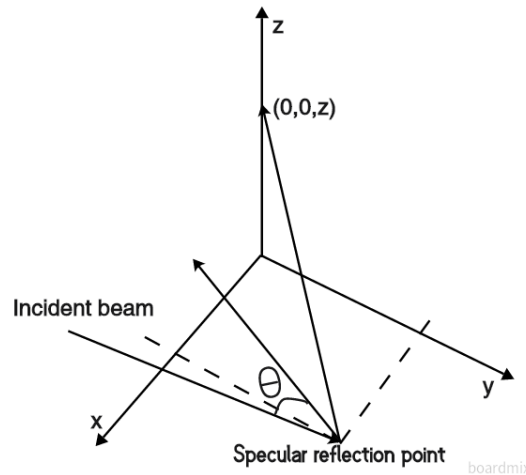
R is the radius of the entire circular area, and r is the open space radius.

Take the maximum loss =2.83%, therefore, take the mean =1.42%.

## 2.2 Cosine efficiency calculation model

Cosine loss refers to the decrease of receiving energy caused by the incident direction of sunlight is not parallel to the normal direction of the mirror lighting port, and the cosine efficiency is the cosine value of the solar incidence Angle, the smaller the solar incidence Angle, the greater the effective area reflected on the heliostat, and the higher the cosine efficiency will be [8]. The cosine efficiency is the point product between the incident direction of the solar ray and the normal direction of the reflected position. The size of the incidence Angle depends on the position of the sun, and the position of the sun mainly depends on the Solar hour angle  $\omega$ , the Local latitude  $\varphi$  and the Solar declination angle  $\delta$ .

Take the reflection path of a certain day mirror in the whole as the study object, as shown in Fig 6.



4Figure 6: The heliostat field coordinate system

Let the direction vector of the solar incident light  $\vec{a}$  be.

$$\vec{a} = (\cos a_s \sin \gamma_s, \cos a_s \cos \gamma_s, \sin a_s). \quad (5)$$

$\vec{b}$  is the direction vector of the sun reflecting light.

$$\vec{b} = \left( \frac{-x_b}{(x_b^2 + y_b^2 + (z - z_b)^2)^{\frac{1}{2}}}, \frac{-y_b}{(x_b^2 + y_b^2 + (z - z_b)^2)^{\frac{1}{2}}}, \frac{(z - z_b)}{(x_b^2 + y_b^2 + (z - z_b)^2)^{\frac{1}{2}}} \right) \quad (6)$$

From the reflection law.

$$\cos 2\theta = \vec{a} * \vec{b} \quad (7)$$

$2\theta$  is the Angle between the incoming light and the reflected light.

From the trigonometry function.

$$\cos \theta^2 = \frac{\cos 2\theta + 1}{2} \quad (8)$$

Cosine efficiency can be obtained by combining the above formula  $\eta_{\cos}$ .

$$\eta_{\cos} = \cos \theta. \quad (9)$$

### 2.3. Collector truncation efficiency

The collector receives this energy attenuated, and because the light is tactical, not all light can be reflected on the collector, so it is simplified to parallel light, showing the analysis principle, as shown in Fig 7.

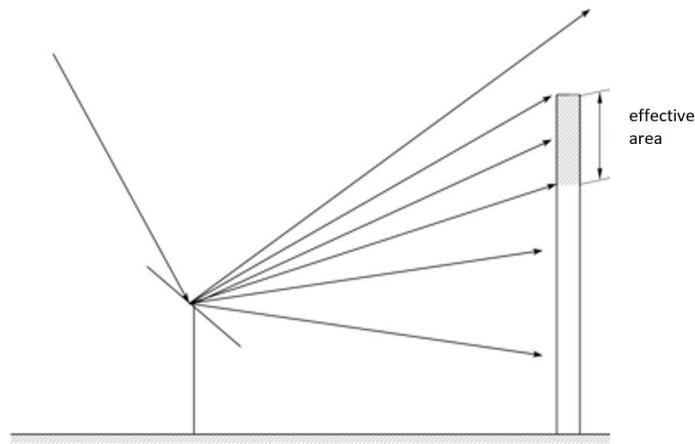


Figure 7: Schematic diagram of the collector truncation efficiency

$$\eta_{\text{trunc}} = \frac{\text{Collectors received energy}}{\text{Specular total reflection energy} - \text{Shadow blocking loss energy}} \quad (10)$$

Collectors received energy = Mirror reflectivity \* DNI \* Daylighting area of heliostat.

Specular total reflection energy = DNI \* Daylighting area of the heliostat.

Shadow blocking loss energy = Shadow loss \* DNI \* Daylighting area of heliostat.

DNI is Direct Normal Irradiance, Mirror reflectivity is 0.92; Daylighting area of heliostat here is  $6 * 6 \text{ m}^2$ .

Therefore, the collector truncation efficiency can be obtained [9].

$$\eta_{\text{trunc}} = \frac{\text{Specular reflectance}}{1 - \text{Shadow blocking loss}} \quad (11)$$

### 2.4 Optical efficiency of the solution

The coordinates of the heliostat mirror center and the distance to the collector center are shown in Table 1.

Table 1: Distance from the mirror center to the collector center

x (m)	y (m)	$d_{HR}$
107.250	11.664	107.8823961
105.360	23.191	107.8821212
102.235	34.447	107.8823018
97.911	45.299	107.8821733
92.440	55.619	107.8824673
.....	.....	.....

The atmospheric transmission rate can be obtained.

$$\eta_{at} = 0.99321 - 0.0001176d_{HR} + 1.97 \times 10^{-8} \times d_{HR}^2 \quad (12)$$

$d_{HR}$  represents the distance between the center of the mirror to the center of the collector.

The change in the distance between the center of the mirror and the center of the collector is shown in Fig 8.

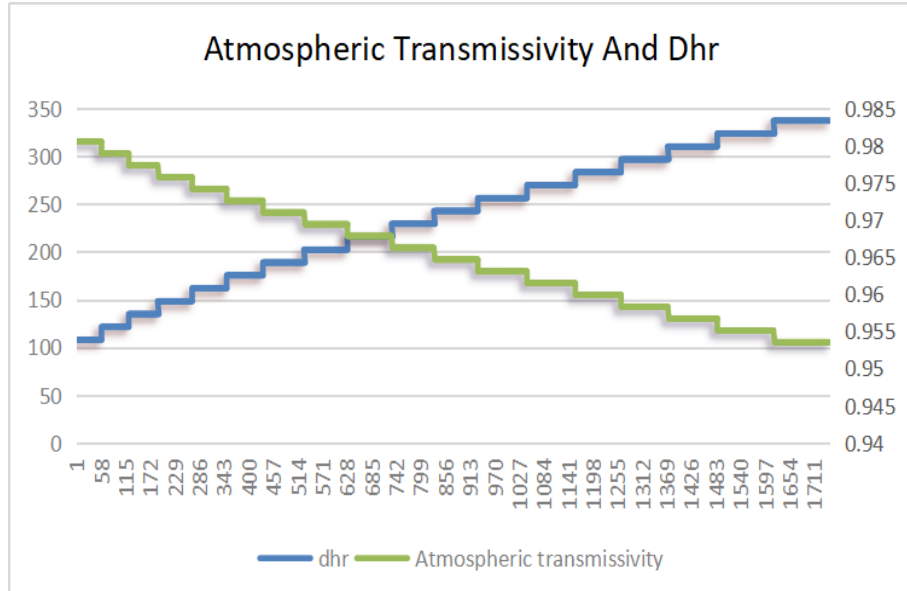


Figure 8: Atmospheric transmittance and  $d_{HR}$

Due to shadow occlusion loss = receiving tower shadow occlusion loss + light transmission occlusion loss + reflected light transmission loss.

The average truncation efficiency and the average shading efficiency can be obtained.

$$\eta_{trunc} = \frac{\text{Specular reflectance}}{1 - \text{Shadow blocking loss}} \quad (13)$$

$$\eta_{sb} = 1 - \text{Shadow blocking loss} \quad (14)$$

Cosine efficiency calculation model.

$$\eta_{cos} = \cos \theta \quad (15)$$

Therefore, the average stage efficiency, the average shadow occlusion efficiency, and the average cosine efficiency of the 21st day of each month are obtained as shown in Table 2.

2Table 2: Corresponds to the average efficiency on the 21 days of each month

date	$\eta_{trunc}$	$\eta_{sb}$	$\eta_{cos}$
On January 21st	0.9402	0.97	0.5916
On February 21st	0.9402	0.97	0.7323
On March 21st	0.9402	0.97	0.8543
On April 21st	0.9402	0.97	0.9299
On May 21st	0.9402	0.97	0.9544
On June 21st	0.9402	0.97	0.9596
On July 21st	0.9402	0.97	0.9114
On August 21st	0.9402	0.97	0.8201
On September 21st	0.9402	0.97	0.6876
On October 21st	0.9402	0.97	0.5512
On November 21st	0.9402	0.97	0.4656
On December 21st	0.9402	0.97	0.4732

## 2.5 Output thermal power solution

Sun Angle  $\omega$  is below:

$$\omega = \frac{\pi}{12} (ST - 12) \quad (16)$$

ST is local time (using a 24-hour clock method).

Sinusoidal value of the Solar Declination Angle is below.

$$\sin \delta = \sin \frac{2\pi D}{365} \sin \left( \frac{2\pi}{360} 23.45 \right) \quad (17)$$

D is the number of days starting from day 0 based on the Spring Equinox.

Since the spring of 2021 is divided on March 20, the calculated values are shown in Table 3 below.

Table 3: D corresponding to the 21st day of each month

1.21	2.21	3.21	4.21	5.21	6.21	7.21	8.21	9.21	10.21	11.21	12.21
-58	-27	1	32	62	93	123	154	185	215	246	276

Know the local latitude of 39.4, the north latitude is positive, and the solar altitude Angle.

$$\sin \alpha_s = \cos \delta \cos \varphi \cos \omega + \sin \delta \sin \varphi \quad (18)$$

Solar azimuth is below.

$$\cos \gamma_s = \frac{\sin \delta - \sin \alpha_s \sin \varphi}{\cos \alpha_s \cos \varphi} \quad (19)$$

Normal direct radiation irradiance DNI is below.

$$DNI = G_0 \left[ a + b \exp \left( -\frac{c}{\sin \alpha_s} \right) \right] \quad (20)$$

$$a = 0.4237 - 0.00821(6 - H)^2 \quad (21)$$

$$b = 0.5055 + 0.00595(6.5 - H)^2. \quad (22)$$

$$c = 0.2711 + 0.01858(2.5 - H)^2. \quad (23)$$

$G_0$  is the solar constant, whose value is 1.366,  $H$  is at an altitude of 3000m.

$$E_{\text{field}} = \text{DNI} \cdot \sum_{i=1}^N A_i \eta_i. \quad (24)$$

$E_{\text{field}}$  is the output thermal power of the heliostat field.  $A_i$  is the daylighting area of the  $i$ -th heliostat.  $\eta_i$  is the optical efficiency of the  $i$ -th mirror.

### 3. Study on the output thermal power of the heliostat field

#### 3.1 Model building

Define the fitness function:  $f(s)$  to a legitimate sequence of cities <sup>[10]</sup>.

$$\bar{s} = (c_1, c_2, \dots, c_n, c_{n+1}). \quad (25)$$

The inverse of the sum of the distances between the two neighbouring cities in this sequence can be used as the fitness of the corresponding individual  $s$ , so the fitness function.

$$f(s) = \frac{1}{\sum_{i=1}^n d(c_i, c_{i+1})} \quad (26)$$

Encode the individual  $s$  and perform genetic operations.

$$\bar{s}_1 = (A, \bar{C}, B, E, D, \bar{A}), s_2 = (A, E, D, C, B, A). \quad (27)$$

Implement routine crossover or variation operations, such as exchanging three digits.

$$s'_1 = (A, C, B, C, B, A), s'_2 = (A, E, D, E, D, A) \quad (28)$$

Or change  $C$  in the second place of chromosome  $s$  to  $E$ .

$$s''_1 = (A, E, B, E, D, A). \quad (29)$$

The sum obtained above are all illegal city sequences.

Chromosome selection-replication is below.

$$P(x_i) = \frac{f(x_i)}{\sum_j^N f(x_j)} \quad (30)$$

$N$  chromosomes are randomly selected from  $S$  in  $N$  times and replicated.

The closer the layout parameter evaluated by the fitness function is to 1, the better the fitness of the parameter, and the evaluation score is 0.7684 0.8456 0.8243 0.9462 0.8642 0.9523 respectively.

### 4. Conclusions

In this paper, the observation analogy method, genetic algorithm and deep multiple search algorithm are used to study the optical efficiency of the heliostatic field and to maximize the average



annual output thermal power of the rated power of the unit mirror area. Results: the absorption tower is located in the center of the circular heliostat field, heliostat size is 6m \* 6m, installation height is 4m, the annual average optical efficiency of the heliostat field is 0.6121, the annual average cosine efficiency is 0.7443, the annual average shadow occlusion efficiency 0.97, annual average cut-off efficiency 0.9404, annual average output thermal power 77.0717 (MW) and annual average output thermal power per unit mirror area 1.2269 (kW/m<sup>2</sup>). At absorber position (0,0), size 7m \* 7 m, the number of faces 1052, total area of heliostat is 51548 (m<sup>2</sup>), annual average optical efficiency of heliostat field 0.6912, annual average cosine efficiency 0.8323, annual average shadow occlusion efficiency 0.98, annual average cutoff efficiency 0.9412, annual average output thermal power 61.1795MW, and annual average output thermal power per unit mirror area 1.0722 (kW/m<sup>2</sup>).

## References

- [1] Zheng-Nong L I , Xiao-Han L , Wei-Xiang W U ,et al. *Research on the Optimization Design of Heliostat Structure Based on Uniform Design and Linear Regression*[J]. *Journal of Hunan University(Natural Sciences)*, 2012, 39(12):1-6.
- [2] Lee K , Lee I . *Optimization of a heliostat field site in central receiver systems based on analysis of site slope effect*[J]. *Solar Energy*, 2019, 193:175-183. DOI:10.1016/j.solener.2019.09.027.
- [3] Hu T , Yu Q , Wang Y S . *Study on layout and optimization of heliostat field in solar tower power plant based on ray trace method*[J]. *Kung Cheng Je Wu Li Hsueh Pao/Journal of Engineering Thermophysics*, 2015.
- [4] Gao Bo, Liu Jianxing, Sun Hao, Liu Erlin, *to optimize the layout of the heliostatic mirror field based on the adaptive gravitational search algorithm* [J]. *Journal of Solar Energy*, 2022,43 (10):119-125.
- [5] O.Farges, J.J.Bezian, M.El Hafi, *Global optimization of solar power tower systems using a Monte Carlo algorithm: Application to a redesign of the PS10 solar thermal power plant* [J], *Renewable Energy*, 2018, 119:345-353.
- [6] Fang Miaosen, Lu Jing, Shen Zhigang, *tower solar helophoscope efficiency modelling and its application* [J]. *Journal of Changzhou Institute of Information Technology*, 2021,20 (03):20-24.
- [7] Mutuberría,A,Pascual, et al. *Comparison of heliostat field layout design methodologies and impact on power plant efficiency*[J]. *Enrgy Proced*, 2015.
- [8] Zeng Jichuan, *research on the thermal efficiency evaluation method of tower solar heat absorber* [D]. *Zhejiang University*, 2021.
- [9] Jianxing Liu. *Modeling and simulation of optical efficiency and optimized layout of tower photothermoelectric station* [D]. *Lanzhou Jiaotong University*, 2022.
- [10] Gu Xiuxiu, Gao Jun, Liu Wenfeng, et al. *Research on multi-objective optimization of signal timing at two adjacent intersections* [R]. *Nanchang: Nanchang University*, 2015.